

COMMISSARIAT A L'ENERGIE ATOMIQUE

CENTRE D'ETUDES NUCLEAIRES DE SACLAY

Service de Documentation
F91191 GIF SUR YVETTE CEDEX

CEA-CONF--8337

L6

CEA - SPHT--86-021

HARMONIC EXCITATIONS IN QUASICRYSTALS

J.M. Luck

CEA CEN Saclay, 91-Gif-sur-Yvette (France). IRF

Communication présentée à : Workshop on aperiodic crystals
Les Houches (France)
11-20 Mar 1986

Résumé - On étudie les excitations harmoniques des quasicristaux (phonons) sur un modèle unidimensionnel simple. Le spectre de ce modèle est un ensemble de Cantor, dont on discute les propriétés d'auto-similarité. Les modes propres sont toujours "critiques", c'est-à-dire ni étendus ni localisés.

Abstract - The harmonic excitations (phonons) of quasicrystals are studied in a simple one-dimensional model. The spectrum is a Cantor set, which exhibits selfsimilarity properties. The eigenstates are generically "critical", i.e. neither extended nor localized.

I - INTRODUCTION

In this communication, I will summarize a recent work in collaboration with Dimitri Petritis [1]. We have chosen to use the well-known projection method [2-5] to generate an almost periodic tiling of the line with two types of tiles, namely short and long segments, of respective lengths $s = \sin \theta$ and $c = \cos \theta$, where θ is the angle between the x-axis and the strip used to construct the tiling (see Figure 1). We shall restrict ourselves to the model defined by the golden mean : $\tan \theta = \tau^{-1} = \frac{1}{2}(\sqrt{5}-1)$.

The harmonic excitations (phonons, tight-binding electronic modes, etc.) are assumed to be described by a Laplace operator involving only nearest-neighbor interactions :

$$(\Delta\varphi)_n = \lambda_n^{-1}(\varphi_{n+1} - \varphi_n) - \lambda_{n-1}^{-1}(\varphi_n - \varphi_{n-1}) \quad (1)$$

where the couplings λ_n are attached to lattice bonds. We define them as depending only on the bond lengths, namely $\lambda_n = \lambda$ for short bonds ($l=s$) and $\lambda_n = \lambda_c$ for long bonds ($l=c$). Choosing units such that $\lambda_c = 1$, we keep $\lambda_s = \rho < 1$ as a free parameter.

The equation obeyed by eigenstates of Δ reads

$$(\Delta+z)\varphi_n = 0 \quad (2)$$

where z denotes the squared eigenfrequency ω^2 in reduced units. Sections II and III of this communication are devoted to the spectrum and the eigenstates of Eq.(2), respectively.

II - THE SPECTRUM

It will be convenient to rewrite Eq.(2) in terms of new dynamical variables Q_n , which live on bonds, and are defined by

$$\begin{aligned} Q_n &= \lambda_n^{-1}(\varphi_{n+1} - \varphi_n) \\ \varphi_n &= z^{-1}(Q_{n-1} - Q_n) \end{aligned} \quad (3)$$

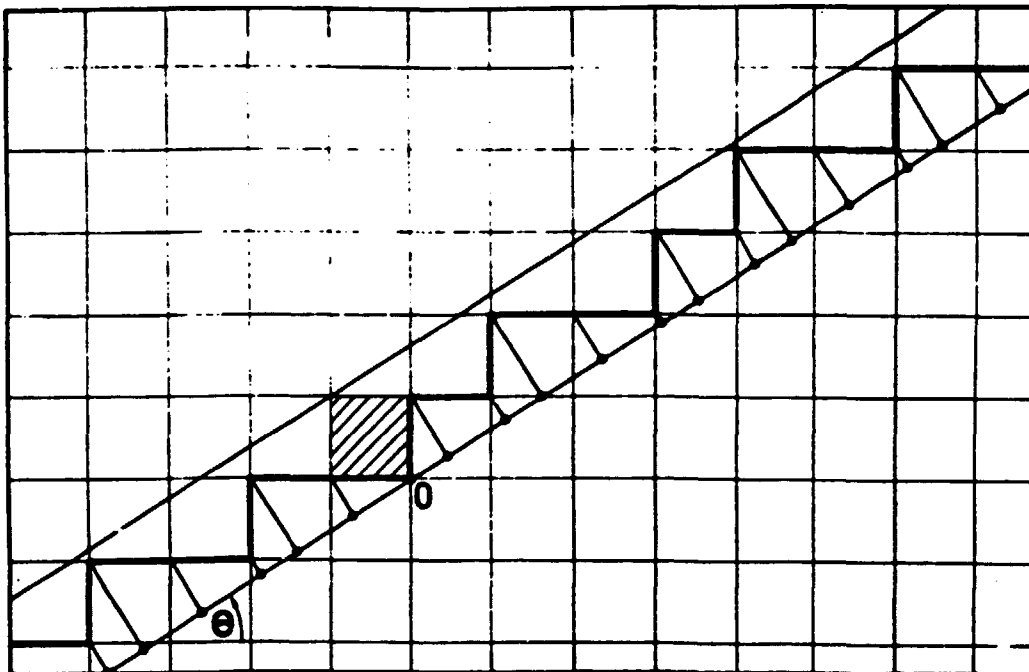


Fig.1 - Construction of a one-dimensional quasicrystal by the projection method.

Eq.(2) can then be recast in the following matrix form :

$$\begin{pmatrix} Q_{n+1} \\ Q_n \end{pmatrix} = \begin{pmatrix} 2-z\lambda_n & -1 \\ 1 & 0 \end{pmatrix} \begin{pmatrix} Q_n \\ Q_{n-1} \end{pmatrix} \quad (4)$$

and hence

$$\begin{pmatrix} Q_{n+1} \\ Q_n \end{pmatrix} = T_n \begin{pmatrix} Q_1 \\ Q_0 \end{pmatrix} \quad (5)$$

where T_n is a product of $(n-1)$ elementary 2×2 transfer matrices.

It can be shown from the geometry of the model that the sequence of matrices T_{F_L} , where F_L are the Fibonacci numbers, defined by $F_0=0$, $F_1=1$, and the recursion relation $F_L = F_{L-1} + F_{L-2}$, obey an exact three-term recursion :

$$T_{F_L} = T_{F_{L-1}} T_{F_{L-2}} \quad (L \text{ odd}) \quad (6)$$

$$T_{F_L} = T_{F_{L-2}} T_{F_{L-1}} \quad (L \text{ even})$$

and hence their normalized traces $x_L = \frac{1}{2} \text{Tr } T_{F_L}$ satisfy

$$x_L = 2x_{L-1} x_{L-2} - x_{L-3} \quad (7)$$

$$x_0 = 1-z/2 ; x_{-1} = 1-\rho z/2 ; x_{-2} = 1.$$

This last property has been used by several authors [6-10] to study Schrödinger equations with almost periodic potentials. In the present situation, this recursion has a simple geometrical origin, and therefore holds for all values of z and ρ .

The study of the mapping (7) shows that the spectrum of Δ is generically a Cantor set. Figure 2 shows a plot of the integrated density of states $H(z)$ for $\rho=1/2$: its Cantor structure is quite apparent. We have shown that (7) has more quantitative consequences, namely the existence of power-law singularities, modulated by periodic

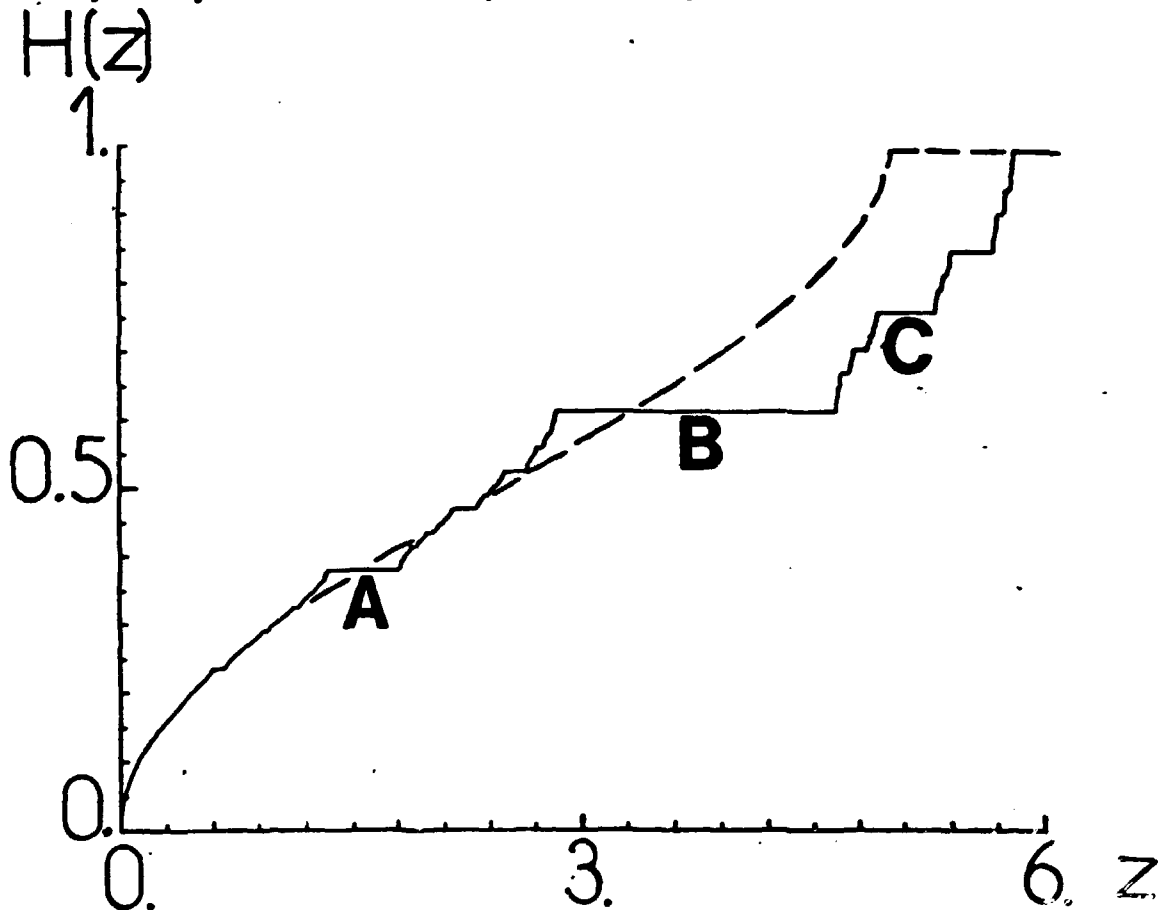


Fig.2 - Plot of the integrated density of states $H(z)$ for $\rho=1/2$ (full curve), and of the underlying average lattice (dashed curve).

amplitudes, in $H(z)$ at each gap edge. In the simple case of the upper bound of the spectrum z_{\max} , our result reads

$$1-H(z) \sim \left(z_{\max}-z\right)^{\Delta} P\left[\ln\left(z_{\max}-z\right)\right] \quad (8)$$

where $\Delta = 0.427174$, and the period of P is $\lambda = 2.252999$. Figure 3 illustrates this behavior.

III - THE EIGENSTATES

The nature of the eigenstates of almost periodic equations is known as a difficult subject. In the present case, we have nevertheless been able to characterize their essential features.

Our main result is that the eigenmodes are neither extended nor localized. The absence of localization in the type of model we consider has been proven rigorously by Delyon and Petritis [11]; we shall not develop their argument presently. The existence of conventional extended states (quasi-Bloch-waves) is a more subtle question, which may depend on the diophantine properties of the slope $\tan \theta$ [12]. A heuristic scaling analysis of the mapping (7) leads us to the following conclusion: the eigenstates have a characteristic length $\xi(\omega^2)$, beyond which they lose the memory of their initial phase. This "memory length" therefore demarcates two regimes: at scales smaller than ξ , an eigenfunction behaves more or less like a plane wave; at scales larger than ξ , its behavior is "critical", and characterized by wild variations in small regions, far apart from each other, on top of a very small background. Moreover, we have argued that $\xi(\omega^2)$ is finite for all non-zero frequencies, but

diverges with an essential singularity at small frequency :

$$\xi(\omega^2) \sim \exp\left[K(\rho)/\omega^2\right] \quad (\omega^2 \rightarrow 0) \quad (9)$$

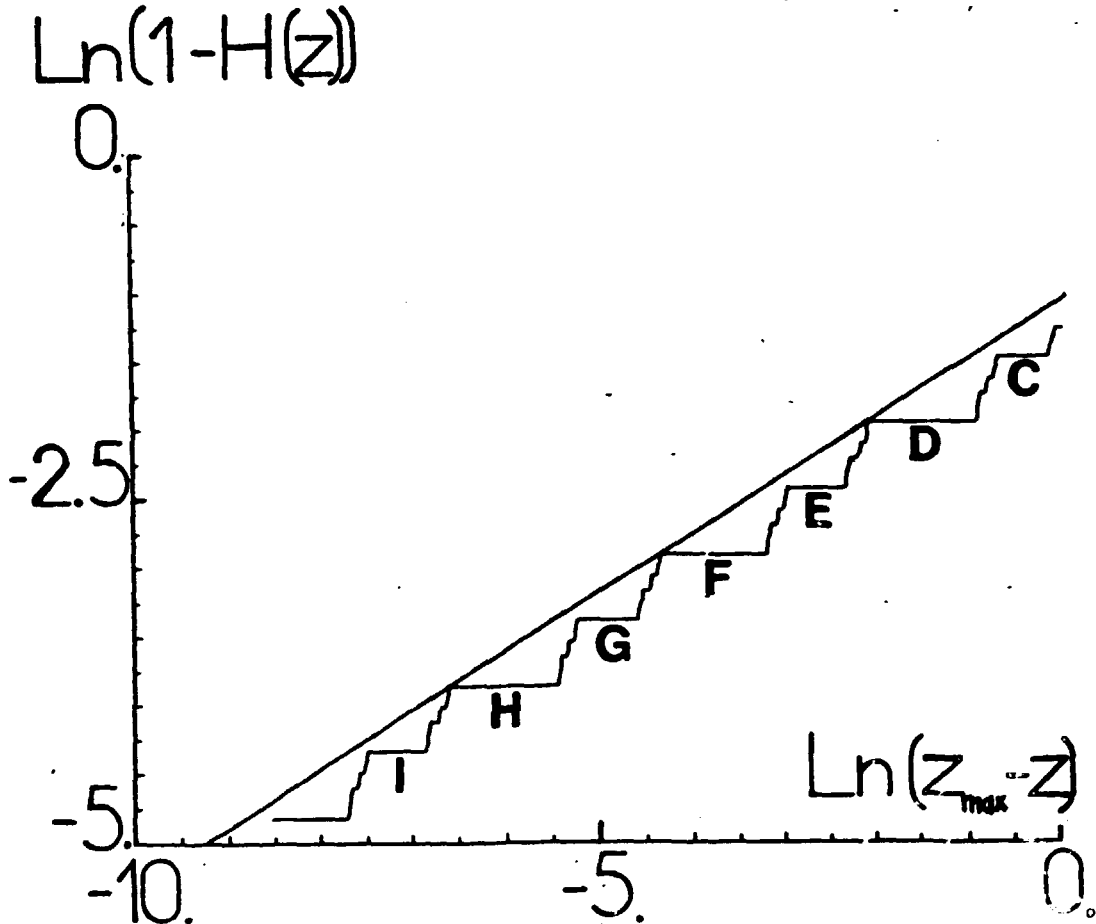


Fig.3 - Log-Log plot of $1-H(z)$ against $(z_{\max} - z)$ for $\rho=1/2$, showing the scaling behavior of the spectrum around its upper bound.

Although the trace mapping (7) is intimately related to the value $\tan \theta = \tau^{-1}$ of the slope, we think that all eigenstates are "critical" for all irrational values of $\tan \theta$ having typical diophantine properties.

We end this section by two illustrations of the strange behavior of the eigenstates. The first one consists in plotting an eigenmode in its phase plane (φ, Q) , where φ and Q are related through Eq.(3). Figure 4 shows the eigenstates number 61 and 620 of a sample of length 1000 (each figure therefore contains 1000 points). In the first case, the memory length is larger than 1000, and the state is close to being a plane wave (ellipse). In the second case, ξ is small, and the state develops a rich structure, both in position space and in its phase plane.

We have also computed the following moments associated with a given mode

$$\mu_\ell = \left(\frac{1}{N} \sum_{n=1}^N \varphi_n^{2\ell} \right)^{1/\ell} \quad (10)$$

where the eigenstate φ on a sample of length N is normalized in such a way that $\mu_1=1$. Localized eigenstates would have $\mu_\ell \sim N^{1-\ell/\ell}$, while extended ones would give rise to finite μ_ℓ as $N \rightarrow \infty$. Figure 5 shows a plot of the moment μ_∞ for all eigenmodes of a sample of length $N = 800$. A very rich self similar structure appears, which is related to that of the density of states (see Figures 2-3). The letters on Figures 2,3,5 are a consistent notation for certain sequence of gaps. The threefold fine structure of each peak of μ_∞ can be explained in terms of a particular six-cycle of the trace mapping (7). The reader is referred to our publication [1] for a more detailed discussion of these phenomena.

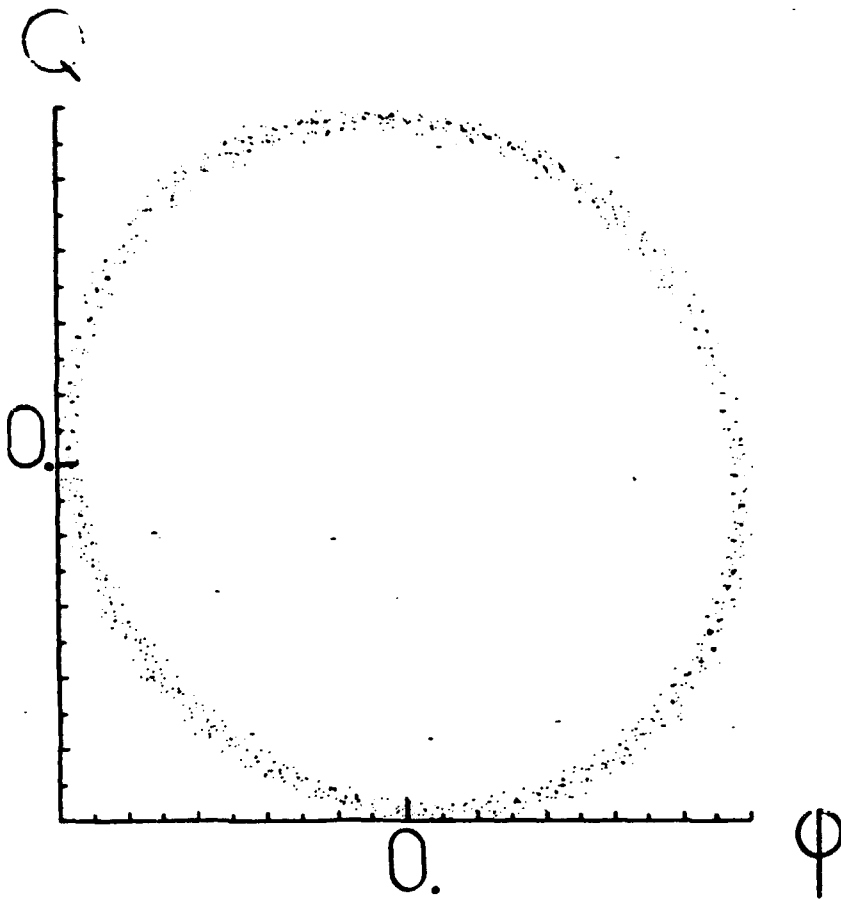


Fig.4a - Representation in its phase plane of the eigenstate number 61 of a sample of size $N = 1000$ sites.

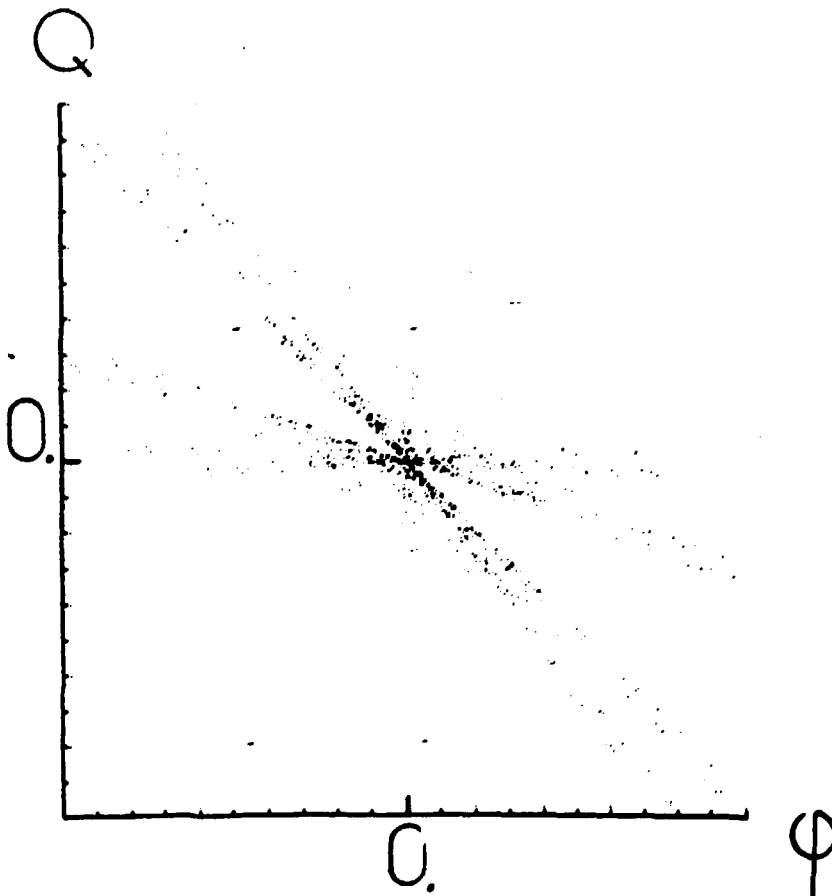


Fig.4b - Same as figure 4a for the eigenstate number 620.

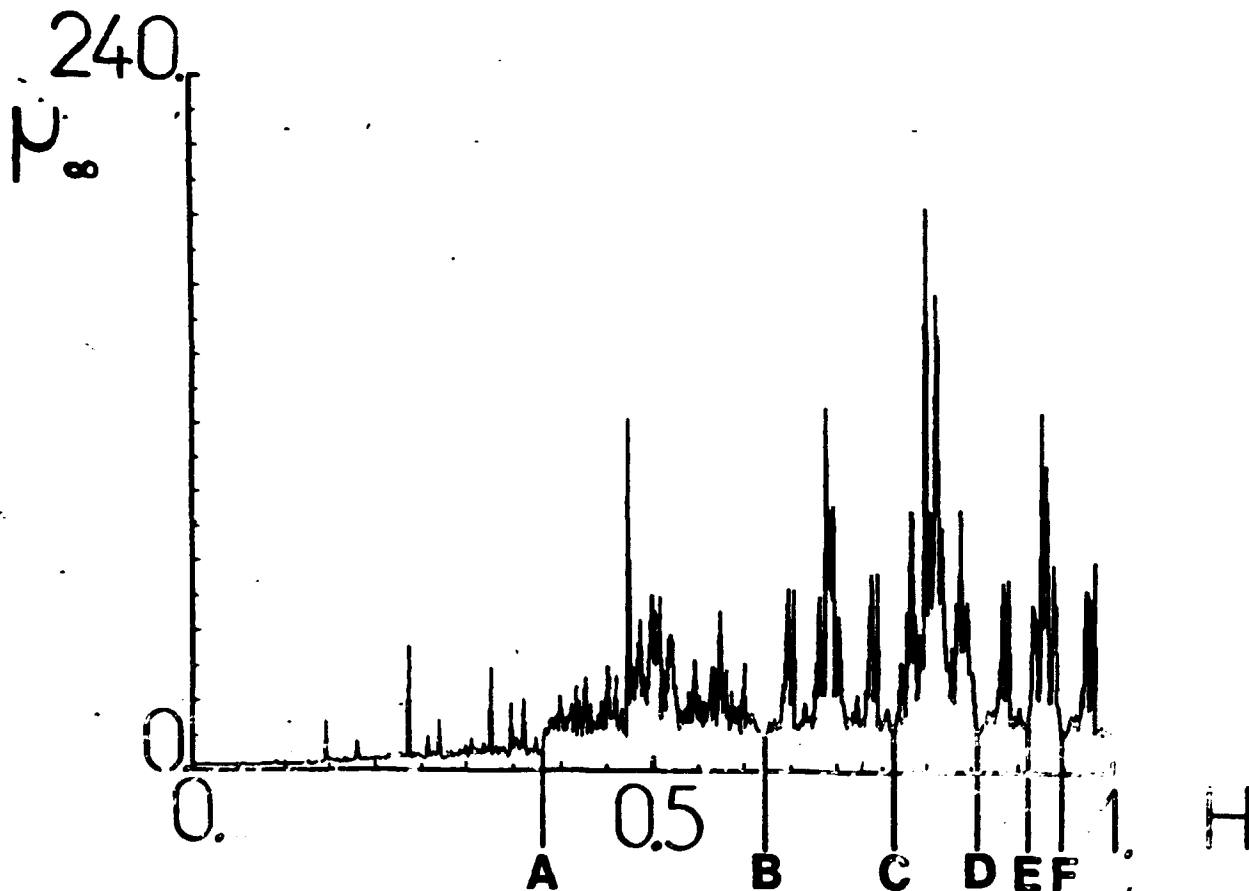


Fig.5 - Plot of the moment μ_∞ defined in Eq.(10) for all eigenstates of a sample of size $N = 800$ sites, ordered according to increasing frequencies.

REFERENCES

- [1] J.M. Luck and D. Petritis, *J. Stat. Phys.* **42**, 289 (1986).
- [2] P. Kramer and R. Neri, *Acta. Cryst.* **A40**, 580 (1984).
- [3] M. Duneau and A. Katz, *Phys. Rev. Lett.* **54**, 2688 (1985).
- [4] R.K.P. Zia and W.J. Dallas, *J. Phys.* **A18**, L341 (1985).
- [5] V. Elser, *Phys. Rev.* **B32**, 4892 (1985).
- [6] M. Kohmoto, P. Kadanoff and C. Tang, *Phys. Rev. Lett.* **50**, 1870 (1983).
- [7] M. Kohmoto, *Phys. Rev. Lett.* **51**, 1198 (1983).
- [8] M. Kohmoto and Y. Oono, *Phys. Lett.* **102A**, 145 (1984).
- [9] S. Ostlund, R. Pandit, D. Rand, H.J. Schellnhuber and E.D. Siggia, *Phys. Rev. Lett.* **50**, 1873 (1983).
- [10] S. Ostlund and R. Pandit, *Phys. Rev.* **B29**, 1394 (1984).
- [11] F. Delyon and D. Petritis, *Comm. Math. Phys.* (in press).
- [12] B. Simon, *Adv. Appl. Math.* **3**, 463 (1982).